Table 1. Effect of CRA and DMBA on growth of transformed clones of 3T3 cells. The CRA concentration was 1 μg/ml. The DMBA concentration for experiments 1 and 2 was 0.001 μg/ml; for experiment 3, it was 0.1 μg/ml. In experiment 2, treatment I lasted 16 days, and treatment II was for 17 days. In experiment 3, treatment I lasted 14 days, and treatment II was for 15 days.

Treatment	Transformed clones per plate (No.)*		
	Expt. 1	Expt. 2	Expt. 3
Control	16	9 (8–10)	8 (7–9)
CRA	55	33 (23–44)	43 (37–52)
DMBA	15		5 (3–7)
I-Control, II-CRA		20 (15–26)	56 (53–59)
I-DMBA, II-CRA		18 (16–20)	24 (20–29)

* Average of five plates; range of values in parentheses.

the use of four replicates per set. The virus-transformed cell line was SV40-transformed (*5*) and was plated 24 hours prior to the plating of the untransformed cells. The concentration of CRA had no inhibitory effect on the cloning efficiency or growth of mass cultures of 3T3 cells and caused a slight reduction (11 to 30 percent) in the cloning efficiency of SV40-transformed cells.

These experiments (Table 2) show that the growth potential of a virus-induced neoplastic cell in a population containing a 100-fold excess of untransformed cells is increased to 166 to 179 percent in the presence of CRA. On the other hand, the growth of SV40-transformed cells appeared to be somewhat inhibited by the 3T3 cells in the absence of CRA. Figure 1, C and D, shows a similar experiment with a line of cells transformed sequentially with polyoma and SV40.

The postulated structures of the purified, active tumor-promoting fractions from *Croton tiglium L.* (*1*, *6*) indicate that the molecule contains both hydrophobic and hydrophilic groups, and an interaction with biological membranes is a clear possibility. It is possible that these agents could affect the permeability properties of cell membranes, either by allowing materials not usually capable of entering the cells to enter, or by allowing cell components to leach out. Either or both of these processes could have an influence on control mechanisms of the cell, possibly resulting in tumor formation. It has been found that CRA and other promoting agents prepared in our laboratory result in a release of lysosomal enzymes in vitro from rabbit liver preparations (*7*).

Table 2. Effect of CRA on growth of SV40-transformed cells in mixed culture, as shown by number of transformed clones per 100.

SV40 cells alone			SV40 (100)+3T3 (10,000)		
I	II	III	I	II	III
			Control		
33	38	45	24	19	35
			CRA		
23	29	40	43	33	58
			CRA/control, percent		
70	76	89	179	174	166

The observation that cells in culture can be released from contact inhibition by a tumor-promoting agent that interacts with biological membranes suggests that there may be a similar mechanism in vivo. The primary role of a tumor promoter may be the alteration of the properties of cell membranes. One result is that cells are no longer contact-inhibited by their neighbors. A corollary of this model proposes that membrane properties of cells may exert an important controlling influence over the propagation of neoplastic cells in the presence of untransformed cells and that these membrane properties may have general importance for the induction of the sequence of events that leads to cell division. This theory is supported by the work of several investigators (*8*) who suggested that there may be an intimate relation between cellular contact and the biochemical events necessary for macromolecular synthesis and mitosis.

ANDREW SIVAK
BENJAMIN L. VAN DUUREN
Institute of Environmental Medicine, New York University Medical Center, New York 10016

References and Notes

1. B. L. Van Duuren and L. Orris, *Cancer Res.* **25**, 1871 (1965); B. L. Van Duuren, L. Langseth, A. Sivak, L. Orris, *ibid.* **26**, 1729 (1966); B. L. Van Duuren, A. Sivak, A. Segal, L. Orris, L. Langseth, *J. Nat. Cancer Inst.* **37**, 519 (1966).
2. G. J. Todaro and H. Green, *Proc. Nat. Acad. Sci. U.S.* **55**, 302 (1966).
3. ———, *J. Cell. Biol.* **17**, 299 (1963). The 3T3 cells were supplied by Dr. Todaro.
4. R. Dulbecco and G. Freeman, *Virology* **8**, 396 (1959).
5. G. J. Todaro, H. Green, B. D. Goldberg, *Proc. Nat. Acad. Sci. U.S.* **51**, 66 (1964); G. J. Todaro and H. Green, *Science* **147**, 513 (1965); ———, *Virology* **28**, 756 (1966). Dr. Todaro supplied the SV40-transformed cells.
6. E. Hecker, H. Kubinyi, Ch. V. Szczepanski, E. Harle, H. Bresch, *Tetrahedron Lett.*, **1965**, 1837 (1965).
7. G. Weissmann, W. Troll, B. L. Van Duuren, G. Sessa, *J. Clin. Invest.*, in press.
8. A. Goldé, *Virology* **16**, 9 (1962); E. M. Levine, Y. Becker, C. W. Boone, H. Eagle, *Proc. Nat. Acad. Sci. U.S.* **53**, 350 (1965); see also refs. 2 and 5.
9. Supported by NIH grants CA-08580 and ES-00260 (formerly ES-00014 and CA-06989).

31 July 1967

Quartz: Extreme Preferred Orientation Produced by Annealing

Abstract. *Annealing of samples of flint under high pressure, after hot-working in the β-quartz stability field, produced an exceedingly strong concentration of c-axes parallel to the direction of compression. A specimen deformed under identical conditions, but not annealed, exhibited a much weaker orientation. The strength of the annealed orientation rivals that of the remarkable "cube texture" produced by annealing some face-centered cubic metals after extreme reduction by rolling.*

Quartz rocks deformed under metamorphic conditions in nature recrystallize into aggregates with moderate-to-high preferred orientations. The highest concentration of *c*-axes reported is 37.5 percent per 1 percent area (*1*). A comprehensive experimental study of the development of preferred orientation in quartz aggregates (*2*, *3*) has found that recrystallization of flint *during* compression under high temperatures and pressures produces two types of preferred orientations (Fig. 1) (*3*). The conditions under which these orientations are developed will be reported separately. Many recrystallized flints are too fine-grained for measurement with conventional universal-stage techniques and are being investigated with x-ray methods (*4*), together with photometric optical analysis (*5*), in my laboratory. These studies reveal orientations similar to those in Fig. 1.

In contrast to these weak-to-moderately strong preferred orientations produced in "syntectonic recrystallization," the extremely strong orientation that I now report was formed by *annealing* of a hot-compressed flint specimen at hydrostatic pressure. Two cylindrical samples of flint were shortened by 34 percent at 750°C, under a 6-kb confining pressure, at a strain-rate of 0.8×10^{-5} sec^{-1}, in the field of β-quartz stability. Specimen DT-459 (Fig. 2, left) was not annealed,

while DT-460 (Fig. 2, right) was annealed 48 hours at 900°C under a 6-kb hydrostatic pressure. The specimens were in a pronounced temperature gradient due to the cooling effect of the pistons.

X-ray analysis of specimen DT-459 reveals that it has a primary concentration of *c*-axes (7 times random) parallel to the direction of compression (σ_1) and a secondary concentration (1.5 times random) normal to σ_1 (*6*). The porphyroblasts (Fig. 2, left) appear to be less well-oriented than the groundmass, but both types of *c*-axis orientation are represented. The x-ray analysis averages porphyroblasts and groundmass according to their respective projected areas. The central, hotter region of the annealed specimen, DT-460, is more strongly oriented than it is in DT-459, and there is a band of extremely high orientation slightly below the center. The center of this band is shown between crossed polarizers in Fig. 3 (left and right), with polarization parallel and at 45 deg to the direction of compression, respectively.

Most grains in this region are large enough to permit measurement of the *c*-axis orientation on the universal-stage. The measured fabric appears in Fig. 4a. The maximum concentration of *c*-axes is more than 100 times that of a uniform distribution, and is

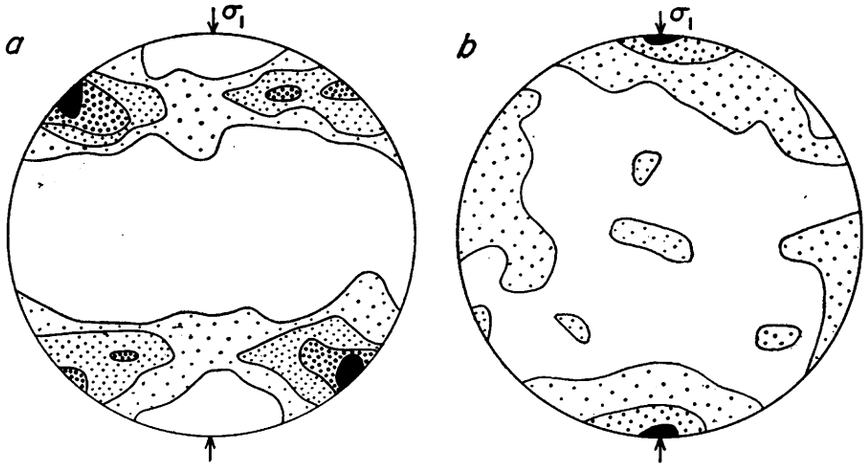

Fig. 1. Typical preferred orientations of quartz *c*-axes in flint recrystallized during deformation at high pressure and temperature, measured microscopically with a universal stage. Strain-rate 10^{-6} sec^{-1}. (a) Shortened 29 percent at 15-kb confining pressure, 800°C. Contours: 4, 3, 2, 1 percent per 1 percent area; 516 *c*-axes (α-field). (b) Shortened 23 percent at 8 kb, 900°C. Contours: 5, 3, 1 percent per 1 percent area; 500 *c*-axes (β-field).

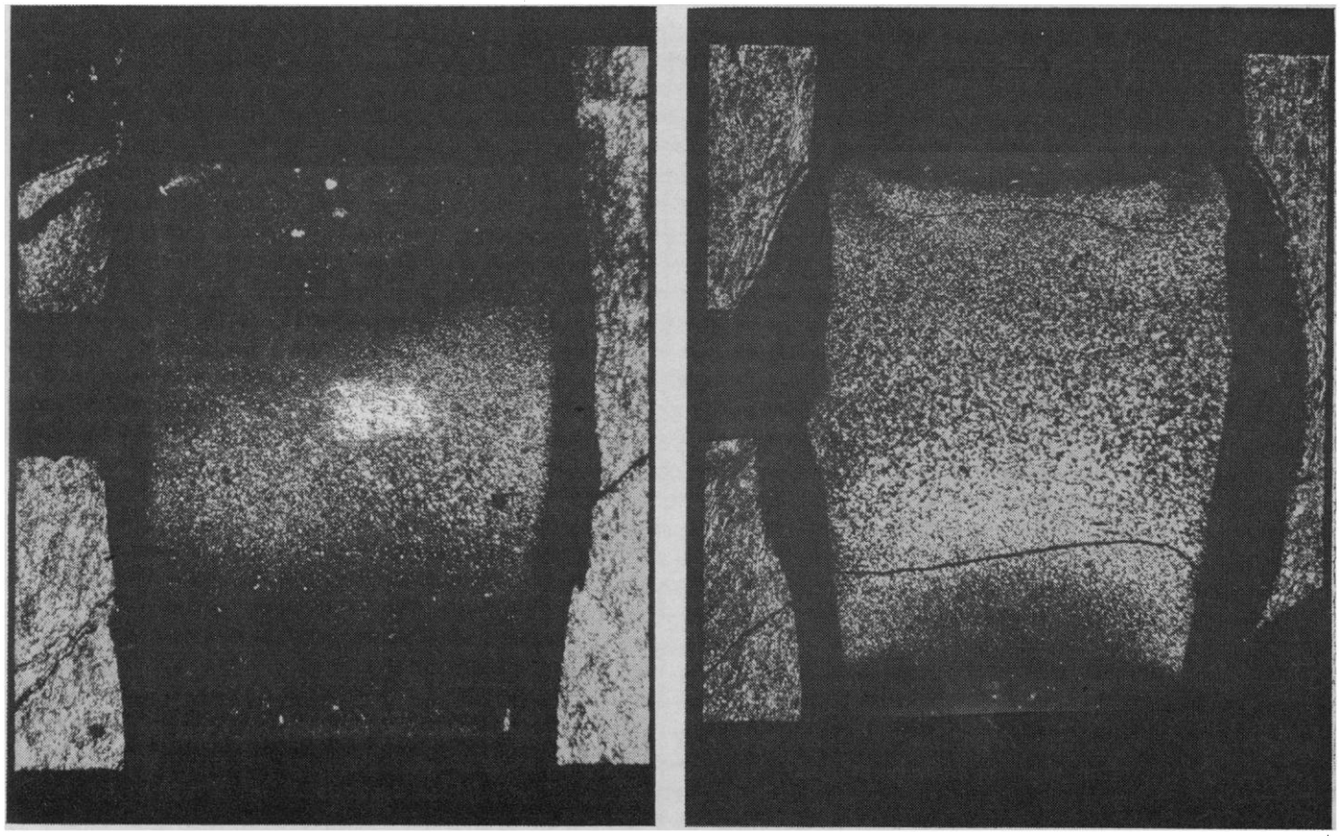

Fig. 2. Photomicrographs of thin-sections of deformed flint cylinders (crossed polarizers). Each 5-mm long specimen is encased in a graphite furnace surrounded by the talc-confining medium. Horizontal black feature to left of specimen marks thermocouple position. (Left) Specimen DT-459, shortened 34 percent at 750°C, 6-kb confining pressure. Central two-thirds of specimen recrystallized to a very fine-grained (~0.005 mm) matrix with porphyroblasts (large crystals) in the middle. Preferred orientation moderate. (Right) Specimen DT-460, also shortened 34 percent at the same conditions, then *annealed* at 900°C, 6-kb hydrostatic pressure. Specimen thoroughly recrystallized to much coarser grained (~0.03 mm) equigranular aggregate. Preferred orientation very strong throughout, with extreme orientation developed in bright area below center of specimen.

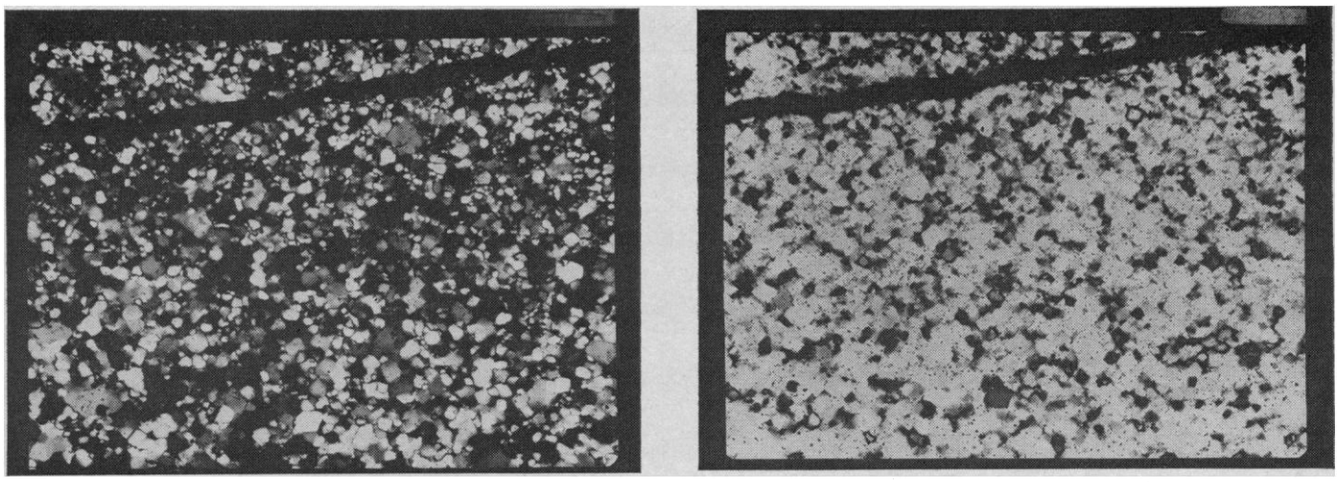

Fig. 3. Region of DT-460 (Fig. 2, right) with the highest preferred orientation (crossed polarizers). High degree of orientation shown by difference with polarization parallel (left) and at 45 deg (right) to direction of compression. Note equidimensional, polygonal grains. Fields of view 0.9 mm across.

parallel to the direction of compression (Fig. 4b); 50 percent of the *c*-axes lie within 6.4 deg of this direction. The smaller grains, whose *c*-axis orientation could not be measured, are not as strongly oriented as the others; they could perhaps as much as halve the maximum concentration of *c*-axes. However, unlike that in DT-459, there is definitely no orientation component with *c*-axes perpendicular to σ_1. This experiment has been repeated with similar results.

We have no satisfactory explanation of the development of this very high preferred orientation, which appears analogous to the "cube texture" developed in some face-centered cubic metals in that annealing produces a much stronger orientation than was developed during deformation (*7*). In these metals a very strong preferred orientation is produced by 80- to 95-percent reduction by cold rolling; concentrations 15 times random have been observed in 111 pole figures (*8*). The cube texture develops upon annealing and is related to the prior orientation by a rotation of ~40 deg about a [111] pole. It has been proposed that the reorientation develops by selective growth of grains which by reason of their orientation have the most mobile grain boundaries relative to preexisting neighboring grains (*9*).

This explanation is less plausible in the present experiments since the 34-percent compression produces a weaker orientation than that which leads to "cube texture." Moreover, the direction of the maximum preferred orientation of *c*-axes in these quartz specimens

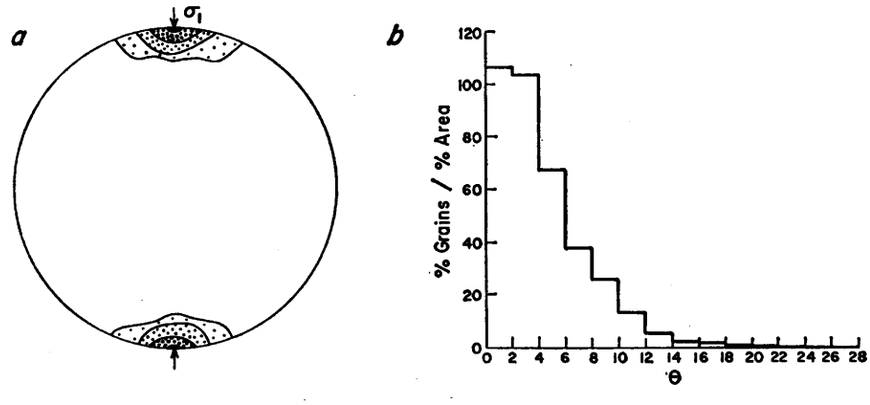

Fig. 4. Preferred orientation of 200 *c*-axes from region in Fig. 3. (a) Standard diagram. Contours: 50, 30, 10, 1 percent per 1 percent area. Maximum concentration in conventional 1 percent solid angle is 60 percent. (b) Frequency distribution histogram normalized so that the ordinate reads in multiples of uniform distribution. The inclination of *c*-axes to σ_1 in degrees is given by θ.

does not change with annealing. In some hexagonal close-packed metals, orientation after annealing is related to orientation produced during cold-work by a 30-deg rotation about the *c*-axis (*10*). There was no significant change in the strength of the orientation. Thus, it is not clear that the "oriented growth" mechanism is the cause of the strong fabric developed by annealing in DT-460. It seems likely, however, that this effect is related to grain growth in some as yet unknown way.

The significance of this phenomenon in the development of natural quartz fabrics is not yet clear. For example, preliminary experiments indicate that the process is not restricted to β-quartz, but that annealing can also change the type of preferred orientation developed in α-quartz. The fact that such a phenomenon exists in rocks as well as in metals strongly suggests to me that geologists must consider processes of development of preferred orientation other than the three that have received most attention in the literature: (i) growth of crystals in orientations thermodynamically favored by considerations of elastic strain energy under nonhydrostatic stress, (ii) orientation of crystals by rotation due to intracrystalline glide, and (iii) orientation by rigid-body rotation of flat or elongate grains.

These experiments provide evidence that high orientations may be produced by recrystallization under hydrostatic stress after suitable deformation. The mechanism therefore is clearly different from the three hypotheses listed.

H. W. GREEN II
Institute of Geophysics and Planetary Physics, University of California, Los Angeles

References and Notes

1. A. Kvale, *Norsk Geol. Tidsskr.* **25**, 193 (1945).
2. N. L. Carter, J. M. Christie, D. T. Griggs, *J. Geol.* **72**, 687 (1964); C. B. Raleigh, *ibid.* **73**, 369 (1965); D. T. Griggs, J. S. Starkey, H. W. Green, J. D. Blacic, D. W. Baker, N. L. Carter, J. M. Christie, *Trans. Amer. Geophys. Union* **46**, 541 (1965); B. E. Hobbs, *ibid.* **47**, 494 (1966).
3. H. W. Green, *Trans. Amer. Geophys. Union* **47**, 491 (1966).
4. D. W. Baker, H. R. Wenk, J. M. Christie, in preparation.
5. D. W. Baker, *Trans. Amer. Geophys. Union* **46**, 541 (1965); unpublished results.
6. H. R. Wenk, D. W. Baker, D. T. Griggs, *Science*, this issue.
7. C. S. Barrett and T. B. Massalski, *Structure of Metals*, (McGraw-Hill, New York, ed. 3, 1966), pp. 555–56; 570–72; 579–83.
8. H. Hu and S. R. Goodman, *Trans. Met. Soc. AIME* **227**, 627 (1963).
9. P. A. Beck, *Trans. AIME* **191**, 474 (1951); *ibid.*, p. 475; T. J. Koppenaal, M. N. Parthasarathi, P. A. Beck, *ibid.* **218**, 98 (1960).
10. R. K. McGeary and B. Lustman, *J. Metals* **3**, 994 (1951).

11. Publication No. 594 of the Institute of Geophysics and Planetary Physics. Supported by NSF grant GP5575. B. E. Hobbs' work on deformation and annealing of single crystals of quartz provided inspiration for these experiments. D. T. Griggs and J. M. Christie provided laboratory facilities and helpful discussion. Correspondence with Hsun Hu was stimulating. J. de Grosse prepared the thin sections.

26 June 1967

X-Ray Fabric Analysis of Hot-Worked and Annealed Flint

Abstract. *Two specimens of flint described by Green have been subjected to intensive x-ray fabric analysis. The specimen compressed in the β-quartz field recrystallized to a fabric with a strong maximum of* c*-axes parallel to the direction of compression and a weaker equatorial concentration perpendicular to the axis of compression. Annealing of a similar specimen eliminated the equatorial concentration and strengthened the axial concentration six- to eightfold. In the latter specimen, the fabric determined by x-ray analysis agrees closely with Green's optically measured fabric. It is possible to obtain* c*-axis fabrics directly from the very weak 0003 diffraction peak.*

Green discovered that an extremely strong preferred orientation developed a hot-compressed specimen (DT-460) of Dover flint when it was annealed (*1*). A similar specimen (DT-459) without annealing appeared optically to have a much weaker orientation in the same direction, but the grain-size was so small that universal-stage fabric measurement was impossible. We here give the x-ray fabric data of the fine-grained hot-worked sample, and verify Green's optically determined fabric of the annealed sample.

A modified Philips pole-figure goniometer and diffractometer were used to obtain transmission intensity profiles of suitable diffracting planes in a section 90 μ thick, cut parallel to the direction of compression, and rotated in its own plane. The deformation of the specimens was axially symmetric. Other similarly deformed specimens have exhibited a fabric with axial symmetry. For such a specimen transmission profiles are sufficient to characterize the fabric. Since the specimen is only rotated in its own plane, no absorption correction is necessary. In our case profiles extending from parallel to perpendicular to the compression axis have been used. The large grain-size (~0.03 mm) of the annealed specimen required a further modification of the Philips device to obtain adequate counting statistics. The specimen was relatively rapidly oscillated ±5° about the normal to the plane of the primary beam and to the counter; this procedure provided an integration over lattice planes that are within 5° of being at right angles to the section. The usual method of integration by translating the specimen in its own plane was precluded by the small size of the highly oriented region in the specimen, which was not larger than the beam size (diameter, 1 mm). Oscillation or translation modifications are necessary as soon as there are less than 5000 to 10,000 grains in the irradiated area.

A number of profiles have been measured in both specimens (DT-459: $10\bar{1}0$, $20\bar{2}1$, $10\bar{1}1$, $10\bar{1}2$, $10\bar{1}4$, $11\bar{2}0$, $11\bar{2}1$, $11\bar{2}2$, $11\bar{2}3$, $21\bar{3}1$; DT-460: $20\bar{2}0$, $20\bar{2}1$, $20\bar{2}2$, $11\bar{2}0$, $11\bar{2}2$). Three profiles for DT-459 are shown in Fig. 1. Because of the low intensity of the basal 0003 reflection and its close proximity to the much stronger $11\bar{2}2$ reflection as shown in the powder pattern of Fig. 2a, it has not hitherto been possible to isolate the 0003 peak sufficiently to permit determination of an 0003 pole-figure. The very strong preferred orientation of DT-460 indicated that if the plane normal to the *c*-axis concentration were set at the critical Bragg angle, the 0003 peak would be more intense than the $11\bar{2}2$ peak. This was found to be the case (Fig. 2b). The use of a fine receiving slit on the counter, and careful alignment of the collimator system permitted almost total isolation of the 0003 peak, so that it was possible to measure 0003 profiles in both DT-460 and in DT-459 (Fig. 3). The background in these profiles away from the *c*-axis maxima is mostly instrumental noise. Better electronic circuits are now available than the one we used, so that

Table 1. Measured values of I, I°, and ρ_2 and calculated *c*-axis concentrations parallel to the compression.

Specimen	*hkl*	Relative intensities corrected for background		Concentration given as multiples of uniform distribution	
		I at σ_1	I° random	ρ (*hkl*)	ρ (0001)
DT-459	$11\bar{2}2$	22	110	.40	7.2
	0003	9	2.5	(4.8)	
DT-460	$11\bar{2}0$	11	71	.74	47.8
	$20\bar{2}0$	6	48	.45	36.0
	$20\bar{2}1$	4	30	.50	37.5
	$11\bar{2}2$	4	101	.16	44.0
	0003	25	2.5	(73.0)	
	$20\bar{2}2$	2	32	.22	35.2

Table 2. The *c*-axis concentrations parallel to compression given as multiples of uniform distribution.

Specimen	Optical (U-stage)	X-ray peak-intensity ratio	Inverse pole figure	Normalized *c*-axis profile
DT-459		7.2	7.0	4.8
DT-460	107*	40	46	73

* Only larger grains measured (~0.03 mm).